CrossMark

ORIGINAL RESEARCH PAPER

Online tuning of fractional order fuzzy PID controller in smart seismic isolated structures

Abbas-Ali Zamani[1] · **Saeed Tavakoli**[1] · **Sadegh Etedali**[2] ·
Jafar Sadeghi[3]

Abstract This paper aims at designing an adaptive fractional order fuzzy proportional–integral-derivative controller for seismic control of smart base-isolated structure by means of variable friction dampers (VFD). One main challenge occurs when large displacement of the isolator happens due to near-field motions. To overcome this challenge, a solution is to use VFDs. However, the floor accelerations of the superstructure can increase because of sudden changes in the damper friction force of VFDs. Therefore, a suitable control strategy is desired to handle the displacement of isolator without any increase in superstructure acceleration responses during both far-field and near-field earthquakes. First, a sub-level fractional order fuzzy PID (FOFPID) controller is designed to reduce the isolator displacement without significant increase in roof acceleration based on a multi-objective optimization algorithm. Using an adaptive strategy, the fuzzy rule weights of the FOFPID controller are then tuned on-line based on information sensed from both the earthquake and the building responses. Considering nine important performance criteria and several real-data earthquakes, numerical studies are carried out for a benchmark base-isolated structure equipped with VFDs. Simulation results show the superior performance of the proposed controller in mitigation of seismic responses of base-isolated structure against various types of earthquakes in comparison with other controllers presented in previous researches.

Keywords Adaptive control · Base-isolated structures · Fractional order fuzzy PID controller · Multi-objective optimization · Variable friction damper

✉ Saeed Tavakoli
tavakoli@ece.usb.ac.ir

[1] Department of Electrical Engineering, University of Sistan and Baluchestan, Zahedan, Iran

[2] Department of Civil Engineering, Birjand University of Technology, Birjand, Iran

[3] Department of Chemical Engineering, University of Sistan and Baluchestan, Zahedan, Iran

 Springer

1 Introduction

One of the important attentions of engineers take into account when designing a structure is decreasing jeopardies of damages caused by dynamic loads such as ground motions and severe winds as much as possible. Over the past decades, seismic isolation has been the most popular methodology found to preserve structures and their filling from destructive effects of a catastrophe. However, latest studies suggest that near-field (NF) earthquakes owing to their long duration pulses with peak velocities result in considerable displacements at the isolator of a base-isolated structure (Narasimhan et al. 2006; Ozbulut and Hurlebaus 2010; Ozbulut et al. 2011). Passive, semi-active, and active control devices have already been suggested in order to improve performance of seismic isolated structures against NF earthquakes. Among these methods, semi-active devices have received greater attention recently because of their great adaptability to a wide range of different excitations and low power consumption (Ozbulut et al. 2011; Etedali et al. 2013; Amini et al. 2015).

Piezoelectric friction dampers (PFD) are among the most applicable semi-active control tools for structures. PFDs are categorized in variable friction damper (VFD) family and have had successful applications in smart base-isolated structures. PFDs are made up of smart piezoelectric materials and have a vast application in vibration control of structures because they are light, inexpensive, easily accessed, easily implemented and quick in response. (Chen and Chen 2004; Song et al. 2006; Lu and Lin 2009; Lu et al. 2010).

Proportional integral derivative (PID) controllers have had successful applications in vibration control (Guclu and Yazici 2009; Nigdeli and Boduroğlu 2013). In Gad et al. (2017) and Koo et al. (2015), it is shown that the fractional order PID (FOPID) controller could offer a better performance in vibration control in comparison with the standard PID controller. Various fuzzy controllers have also been proposed for vibration control of smart structures in Guclu (2003), Zhao and Li (2015), and Zamani et al. (2017).

Recently combining fuzzy logic controller with fractional order math has grabbed attention as to be instrumental (Das et al. 2012; Sharma et al. 2014; Mishra et al. 2015; Arya and Kumar 2016). Das et al. (2012) used of genetic algorithm (GA) to tune the controller's parameters of a fractional order fuzzy PID (FOFPID) controller. This control strategy has successfully been applied to a delayed nonlinear system and a delayed unstable system. This research has shown that in most cases the fractional order version of fuzzy PID controller performs better than the standard fuzzy PID controller.

FOFPID control has also been applied to a two-link planar robotic manipulator by Sharma et al. (2014). That research suggested that, in terms of performance, the FOFPID controller takes over PID, FOPID, and fuzzy PID controllers. For controlling a chemical distillation column, Mishra et al. (2015) proposed a FOFPID controller which showed better performance over the integer version as well. Arya and Kumar (2016) designed a FOFPID controller for automatic generation control of multi-area multi-source electric power generating system. The FOFPID controller, for which the fractional parameters are designed based on bacterial foraging optimization algorithm, proved outstanding performance in comparison to PID, FOPID, and fuzzy PID. Despite a vast majority of research being conducted on successful application of FOFPID, showing its dominance over PID, FOPID, and fuzzy PID, there is still no examination of this method on vibration control something that we target in current research.

The main goal of seismic control in base-isolated buildings is to decrease the isolation displacement without increasing the acceleration of superstructure. Thus, a trade-off between these conflicting objectives should be made in the design process. In this paper, an adaptive fractional order fuzzy proportional–integral-derivative (AFOFPID) controller is

designed to adjust the contact force of PFDs considering the semi-active control of the benchmark smart base-isolated building during far-field (FF) and NF ground motion. At first a sub-level FOFPID controller is designed using a multi-objective cuckoo search (MOCS) algorithm. Finally, for better consideration of the changes in the frequency content of several earthquakes, an adaptive fuzzy strategy is proposed so that it adaptively tunes the fuzzy rule weights of the sub-level FOFPID controller, according to the roof acceleration and ground velocity. Considering nine performance indices and several real-data earthquakes, the performance of the proposed control strategy is compared to those given by other control strategies.

The rest of the paper is organized as follows. In Sect. 2, the model of a smart base-isolated structure and a piezoelectric friction damper is introduced and discussed. In Sect. 3, to adjust the control force of PFDs in smart base-isolated structures, the proposed control strategy is developed. Numerical simulations and studying results are given in Sect. 4. Moreover, the performance comparison of the proposed controller with several control strategies is presented in this section. At the end, the concluding remarks are summarized.

2 System modeling

2.1 Base-isolated structure model

The dynamic equation of motion of an n-degree of freedom base-isolated structure is given by

$$M\ddot{x}(t) + C\dot{x}(t) + Kx(t) = Du(t) - Mr\ddot{x}_g(t) \qquad (1)$$

where M, C and K are n-by-n mass, damping and stiffness matrices, respectively, and $x(t)$, $\dot{x}(t)$ and $\ddot{x}(t)$ refer to displacement vector, velocity vector and acceleration vector, respectively. The earthquake ground acceleration is denoted by $\ddot{x}_g(t)$. Also, $u(t)$ is the control force applied to the structure. The location matrix for the applied control force and the location vector for the applied dynamical load are denoted by D and r respectively. Reforming Eq. (1) through straightforward math results in the following state equation:

$$\dot{z}(t) = Az(t) + Bu(t) + H\ddot{x}_g(t) \qquad (2)$$

where

$$z(t) = [x(t) \quad \dot{x}(t)]^T, \ A = \begin{bmatrix} 0 & I \\ -M^{-1}K & -M^{-1}C \end{bmatrix}, \ B = \begin{bmatrix} 0 \\ M^{-1}D \end{bmatrix}, \ H = \begin{bmatrix} 0 \\ -r \end{bmatrix} \qquad (3)$$

In Eq. (3), 0 and I denote zero and identity matrices, respectively. To investigate closed-loop performance of the AFOFPID controller, a benchmark five-story base-isolated building, studied in Johnson et al. (1998) is taken into account. The building is considered as a lumped-mass structural model with six degrees of freedom. All the model parameters including structural parameters and isolator parameters are denoted in Table 1 for this benchmark.

The isolation system is built of low-damping rubber bearings. The fundamental period and the damping ratio of the structure without isolator are 0.3 s and 2%, respectively. In fundamental mode, period and damping ratio of the base-isolated structure are 2.5 s and 4% respectively.

Table 1 Isolator and structure parameters. (Reproduced with permission from Johnson et al. 1998)

	Isolator	Floors of structure				
Floor mass (kg)	$m_b = 6800$	$m_1 = 5897$	$m_2 = 5897$	$m_3 = 5897$	$m_4 = 5897$	$m_5 = 5897$
Stiffness values (kN/m)	$k_b = 232$	$k_1 = 33732$	$k_2 = 29093$	$k_3 = 28621$	$k_4 = 24954$	$k_5 = 19059$
Damping coefficients (kN′s/m)	$c_b = 7.45$	$c_1 = 67$	$c_2 = 58$	$c_3 = 57$	$c_4 = 50$	$c_5 = 38$

2.2 Piezoelectric friction damper model

Piezoelectric friction dampers are modern semi-active control devices utilizing piezo-electric actuators for regulating the damping force in order to provide a desired level of friction force. The power consumption of a PFD depends on its command voltage and electric current. The parameters of the piezoelectric friction damper used in this manuscript is based on the experimental studies carried out in Lu and Lin (2009), Lu et al. (2010). As mentioned in these references, the electric current required for a piezoelectric actuator is in the range of several milliAmperes, which is a feasible range to supply a semi active device (Lu and Lin 2009; Lu et al. 2010). The equation representing friction force of a PFD is usually given using sign function as

$$N(t) = N_{pre} + C_{PZ}V(t) \tag{4}$$

$$u(t) = \mu_d N(t)sgn(\dot{x}_b), \; \dot{x}_b \neq 0 \tag{5}$$

$$-\mu_d N(t) \leq u(t) \leq \mu_d N(t), \; \dot{x}_b = 0 \tag{6}$$

where $N(t)$, N_{pre}, C_{PZ} and $V(t)$ are the total contact force, the pre-compressor force, the PFD's piezoelectric coefficient, and the activated voltage of the piezoelectric actuator, respectively. u and μ_d are the damper friction force as well as the friction coefficient between the friction pad and friction bar, respectively. Also, $sgn(\dot{x}_b)$ refers to the sign of the sliding velocity of the isolator, in which the latter means the difference velocities between ground and isolation level. A friction damper has mainly two possible motion modes that are sticking and slipping phases and the thorough behavior of friction force can be described by combining both of these phases. The sliding velocity is non-zero in the slip phase and by Eq. (5) the friction force is obtained. However, in the stick phase, the sliding velocity is equal to zero, i.e. two friction plates have no relative motion and are stuck. The absolute friction force is less than the PFD's maximum friction force. The absolute friction force is usually evaluated through solving for the structure's equations of motion. Schematic diagram of the PFD components is shown in Fig. 1. The parameters related to the PFD, which are used in the simulations are denoted in Table 2.

3 Proposed adaptive control strategy for smart base-isolated structures

The effectiveness of an FOFPID controller essentially depends on the values of the parameters of input–output membership functions (MFs), fuzzy rules, input and output scaling factors and the order of the integral and derivative operators. Due to the external
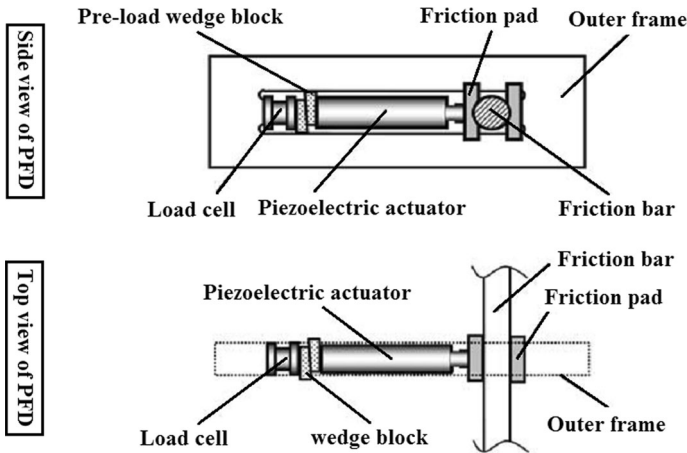
Fig. 1 Side and top view of PFD components. (Reproduced with permission from Lu and Lin 2009)

Table 2 PFD parameters (Reproduced with permission from Lu and Lin 2009)

μ	N_{pre}	C_{PZ}	V_{max}
0.2	1000 (N)	1.10 (N/V)	1000 (V)

excitation uncertainties of smart structures and more importantly the complexity in the mathematical model of them, however, it is a difficult task to obtain the parameters of controller based on analytical methods. In addition, the large displacement of isolator in NF motions is a major challenge that needs to be addressed wisely. One way to overcome this challenge is using PFDs as semi-active devices. On account of semi-active control of a smart base-isolated building using PFDs, however, the floors acceleration of the super-structure can increase owing to sudden changes in the damper friction force of PFDs. A suitable control strategy is demanded that is able to decrease the isolator displacement without allowing the superstructure accelerations to rise during both NF and FF earthquake excitations.

Tuning parameters of an FOFPID controller can be defined as an optimization problem. In fact, here the challenge is to determine appropriate parameters for the controller min-imizing the conflicting performance indices. Multi-objective evolutionary optimization algorithms are the best practice when solving a problem with conflicting objective func-tions and MOCS algorithm is one suitable workaround.

Cuckoo Search (CS) algorithm, introduced by Yang and Deb (2009), is able to effi-ciently handle complex optimization problem with high accuracy and acceptable conver-gence rate. The CS applies Lévy flights, which are more efficient than simple random walks, and can provide a balance between local and global search explorations. Moreover, in comparison to other optimization algorithms the CS has fewer algorithm-dependent parameters. The CS algorithm is configured through altering algorithm parameters that include the population size n, switching probability p_a, step-size α and the Lévy flights exponent β. Unlike α and β, which, in most problems, are assigned constant values of 0.1 and 1.5, p_a and n have greater effects on the algorithm performance as the main design variables (Yang and Deb 2009; Rajabioun 2011). Yang and Deb (2013) presented an

MOCS algorithm for the time when the optimization problem has several conflicting objectives. The performance of MOCS algorithm was examined in comparison to several well-known multi-objective optimization algorithms including NSGA-2. It was shown that the convergence rate of MOCS was the fastest and it led to more accurate solutions (Yang and Deb 2013).

In order to implement the control strategy, an artificial ground acceleration that is generated by passing a Gaussian white noise through a filter, is used. This filter was given in Eq. (7) and introduced in Nagarajaiah and Narasimhan (2006).

$$G_r(s) = \frac{4\xi_g \omega_g s}{s^2 + 2\xi_g \omega_g s + \omega_g^2} \tag{7}$$

where ξ_g and ω_g are the damping and frequency of ground, respectively. For numerical simulations in this study, ξ_g and ω_g are 0.3 and 2π rad/s, respectively. The output of this filter simulates the earthquake which is then used in the optimization procedure.

The FOFPID controller, which is shown schematically in Fig. 2, with $\{K_e, K_d\}$ and $\{K_{PI}, K_{PD}\}$ being its input and output scaling factors respectively, has successful control applications (Das et al. 2012; Sharma et al. 2014; Mishra et al. 2015; Arya and Kumar 2016). Also the block diagram of sub-level FOFPID controller for base-isolated structure equipped with PFDs is shown in Fig. 2.

The actuation voltage of PFDs is the control input and the structure of sub-level FOFPID controller is described in the following. Five membership functions are considered for inputs and the output of the fuzzy logic controller (FLC). Five membership functions of output {ZR, S, M, L, VL}, which are represented by the indexes {0, 1, 2, 3, 4}, denote for zero, small, medium, large and very large respectively. The FLC's output signal is defuzzified using the center of gravity method. An MOCS optimizer is used for simultaneously tuning of six parameters of fractional order part of controller, K_e, K_d, K_{PI}, K_{PD}, λ and μ, 25 fuzzy rules, $I_j, j = 1, \ldots, 25$, and 15 centers of triangular membership functions, $P_{k,z}, k = 1, 2, 3, z = 1, \ldots, 5$. The main issue is to determine the following design vector that minimizing the conflicting performance criteria.

$$d_v = [K_e, K_d, K_{PI}, K_{PD}, \lambda, \mu, I_1, \ldots, I_{25}, P_{1,1}, \ldots, P_{3,5}]^T \tag{8}$$

To obtain a good trade-off between the displacement of isolator and the acceleration of superstructure floors, the design problem is formulated as a multi-objective optimization
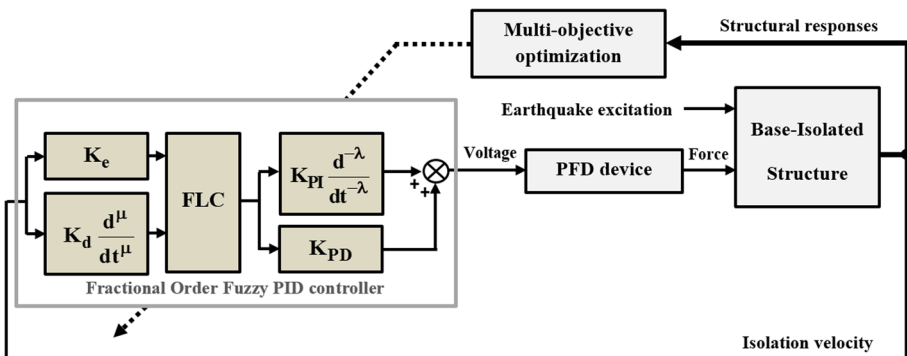

Fig. 2 Block diagram of sub-level FOFPID controller

problem, using sub-level FOFPID controller in Fig. 2 with the following objective functions.

$$\text{Minimize } f_1(d_v) = \frac{\max_t \left\| x_b^{\text{controlled}}(t) \right\|}{\max_t \left\| x_b^{\text{uncontrolled}}(t) \right\|}, f_2(d_v) = \frac{\max_{t,f} \left\| a_f^{\text{controlled}}(t) \right\|}{\max_{t,f} \left\| a_f^{\text{uncontrolled}}(t) \right\|} \qquad (9)$$
$$\text{subject to } L \leq d_v \leq U$$

where $f_1(d_v)$ and $f_2(d_v)$ are the normalized maximum base displacement and normalized peak floor accelerations, respectively. In this equation, a structure with no control tool and control force is considered as an uncontrolled structure. Values L and U are the lower and upper bounds of sub-level FOFPID controller parameters. The lower and upper bounds of each FOFPID controller parameters are $0 \leq K_e, K_d \leq 1$, $0 \leq K_{PI}$, $K_{PD} \leq 2$, $0 \leq \lambda$, $\mu \leq 2$, $0 \leq I_j < 5$, $-1 \leq P_{1,z}$, $P_{2,z} \leq 1$ and $0 \leq P_{3,z} \leq V_{max}$, where $V_{max} = 1000$ refers to the maximum actuation voltage of PFD. To design the proposed controller for seismic control of a smart base-isolated structure equipped with PFDs system, the integer-order approximate transfer function of fractional order integral and derivative part of the sub-level FOFPID controller is calculated using Oustaloup method (Oustaloup et al. 2000). The parameters used in Oustaloup approximation are $\omega_l = 0.01$, $\omega_h = 100$ and N = 6. Also, the simulation time span is 50 s.

Simulation of the base-isolated structure equipped with PFDs is performed subject to the artificial earthquake in Eq. (7). The parameters of the sub-level FOFPID controller are determined using an MOCS optimizer and Fig. 3 shows the set of Pareto-optimal solutions. The population size n and the discovery probability p_a are chosen to be n = 20 and $p_a = 0.5$, respectively. It is worth mentioning that each member of the set of Pareto-optimal front is a possible solution. The desired controller should be able to minimize the isolation displacement while causes no significant increase in the acceleration response of the superstructure. In other words, the best controller should offer the best trade-off between these two conflicting objectives. The input signal of the sub-level FOFPID controller must be selected from different structural responses. In seismic control of base-isolated buildings, the structural responses of isolation system are important. Hence, three candidate
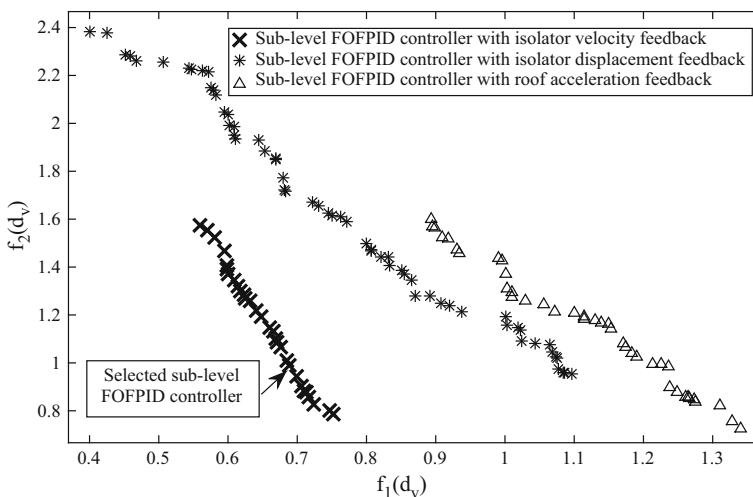

Fig. 3 Set of pareto front for sub-level FOFPID controller design using different feedbacks

feedbacks, i.e. the isolation displacement, isolation velocity, and roof acceleration, are considered. The best input for sub-level FOFPID controller can be determined based on the resulting Pareto optimal front. In the solution proposed, the optimal fuzzy rules and the input and output scaling factors and the fractional order operator parameters are listed in Tables 3 and 4, respectively. Also the optimal parameters of inputs and the output membership functions for sub-level FOFPID controller are shown in Fig. 4. The velocity profile of the ground provides information regarding the ground motions' characteristics. Thus, it is considered as an effective way to improve the performance of the sub-level FOFPID controller where both NF and FF earthquakes might happen.

The block diagram of the AFOFPID controller for smart base-isolated structures equipped with PFDs is illustrated in Fig. 5.

The ground velocity and roof acceleration are two inputs of the fuzzy weighing system. The ground velocity is adopted to reflect the effects of the earthquake. The larger values of the ground velocity indicate seismic excitations with NF characteristics, which usually increase isolator displacement of the structure and need larger damping force. An NF earthquake usually causes large displacement at the base and any attempt to decrease the base displacement often results in increasing the roof acceleration unwillingly. When the absolute value of roof acceleration is increased, the smaller damping forces are needed. To ensure that the proposed controller considers the reduction of the roof acceleration and performs effectively during both NF and FF earthquakes, the absolute value of roof acceleration is picked as the second input.

According to the ground velocity and the inverse value of absolute roof acceleration, fuzzy weighting system tunes the rule weightings of the sub-level FOFPID controller so that the isolation performance improves. Generally, the rule weights in a fuzzy controller are either applied to the whole rule or only the rule output (Nauck and Kruse 1998; Karasakal et al. 2013). Here, the second approach is preferred and it is applied using a factor $\alpha \in [0, 1]$ as the output of the fuzzy weighting system. It is then used in Eq. (10) to evaluate ultimate weights.

$$
\begin{aligned}
W_1 &= \alpha \\
W_2 &= 0.5\alpha + 0.25 \\
W_3 &= 0.5 \\
W_4 &= -0.5\alpha + 0.75 \\
W_5 &= 1 - \alpha
\end{aligned}
\tag{10}
$$

According to Table 3, rules with VL, L, M, S, and ZR as output membership functions take W_1, W_2, W_3, W_4, and W_5 as weights. With this selection, in NF earthquakes that need

Table 3 Fuzzy rule base for sub-level FOFPID controller

Fractional derivative of isolator velocity	Isolator velocity				
	NL	NS	ZR	PS	PL
NL	VL (W_1)	VL (W_1)	L (W_2)	VL (W_1)	ZR (W_5)
NS	VL (W_1)	VL (W_1)	L (W_2)	ZR (W_5)	VL (W_1)
ZR	L (W_2)	VL (W_1)	ZR (W_5)	ZR (W_5)	L (W_2)
PS	S (W_4)	ZR (W_5)	S (W_4)	M (W_3)	VL (W_1)
PL	ZR (W_5)	M (W_3)	M (W_3)	L (W_2)	VL (W_1)

NM negative medium; *NS* negative small; *ZR* zero; *PS* positive small; *PM* positive medium

Table 4 Optimal parameters of the fractional part of the sub-level FOFPID controller

K_e	K_d	K_{PI}	K_{PD}	λ	μ
0.53	0.86	0.12	1.2	0.75	0.84
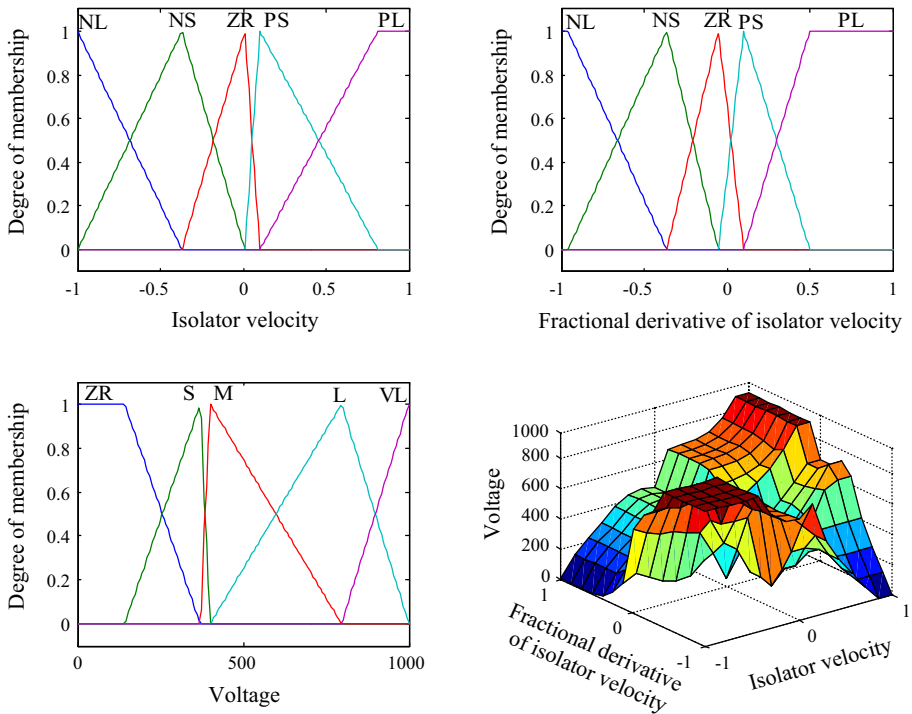
Fig. 4 Inputs and output membership functions for sub-level FOFPID controller
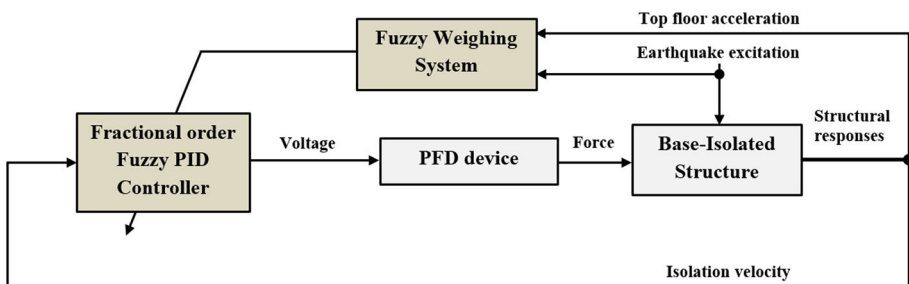
Fig. 5 The block diagram of AFOFPID controller for smart base-isolated structures

larger damping forces, those rules that lead to higher voltage gain will achieve a greater degree of importance because they will have greater weights.

Each fuzzy signal (two inputs, one output) of the fuzzy weighting system is considered to have three membership functions. An MOCS optimizer is used for simultaneously

tuning of input normalization factors, $K_{|\hat{a}|^r}$ and $K_{|\hat{v}|^g}$, nine centers of triangular membership functions and fuzzy rule base. The main issue is to determine the following design vector.

$$d_v = [K_{|\hat{a}|^r}, K_{|\hat{v}|^g}, I_1, \ldots, I_9, P_{1,1}, \ldots, P_{3,3}]^T \tag{11}$$

Optimal parameters of fuzzy weighing system are given in Fig. 6, Tables 5 and 6, respectively.

4 Result and discussion

In order to compare the performance of various control strategies developed for the smart base-isolated structures, a set of important performance indices, as shown in Table 7, and 14 real-data earthquakes are considered (Narasimhan et al. 2006).

A set of 14 real-data earthquake, considered by Narasimhan et al. (2006) in structural control benchmark problem of smart isolated structures, are adopted to examine the generality of the proposed controller.

Simulation analyses of the semi-active control of base-isolated building using PFDs are performed in MATLAB/Simulink. The values of the performance indices, defined in Table 7, are listed in Table 8 for the FP and FN components of earthquakes.

To evaluate the performance of the proposed AFOFPID controller and compare it with maximum passive operation (MPO) of piezoelectric friction dampers, modified clipped-optimal (MCO) controller (Ozbulut et al. 2011), supervisory fuzzy logic controller (SVFLC), self-organizing fuzzy logic controller (SOFLC) (Ozbulut and Hurlebaus 2010), and optimal PID (OPID) controller (Etedali et al. 2013), in reducing the performance indices value J_3, J_5, J_6, J_7 and J_8 are displayed in Fig. 7. It is noted that the FN component
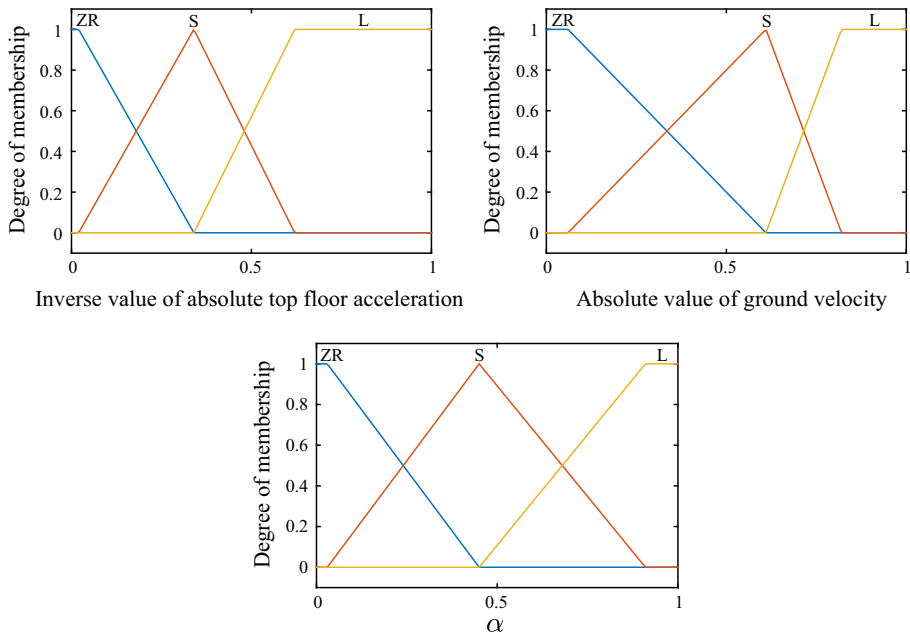

Fig. 6 Inputs and output membership functions for the fuzzy weighing system

Table 5 Fuzzy rule base for the fuzzy weighing system

Absolute value of ground velocity	Inverse value of absolute top floor acceleration		
	ZR	S	L
ZR	ZR	S	S
S	S	S	L
L	L	L	L

Table 6 Optimal input and output parameters of membership functions for fuzzy weighing system

Normalization factor		Parameters of MFs for inverse value of absolute top floor acceleration			Parameters of MFs for absolute value of ground velocity			Parameters of MFs for output of fuzzy weighing system		
$K_{|\ddot{a}|^r}$	$K_{|\dot{v}|^g}$	$P_{1,1}$	$P_{1,2}$	$P_{1,3}$	$P_{2,1}$	$P_{2,2}$	$P_{2,3}$	$P_{3,1}$	$P_{3,2}$	$P_{3,3}$
0.59	0.83	0.02	0.34	0.62	0.06	0.61	0.82	0.03	0.45	0.91

Table 7 Performance evolution criteria

Normalized peak base shear	$J_1 = \frac{\max_t\|V_0(t)\|}{\max_t\|\hat{V}_0(t)\|}$	Normalized peak structural shear	$J_2 = \frac{\max_t\|V_1(t)\|}{\max_t\|\hat{V}_1(t)\|}$
Normalized peak base displacement	$J_3 = \frac{\max_t\|x_b(t)\|}{\max_t\|\hat{x}_b(t)\|}$	Normalized peak inter story drift	$J_4 = \frac{\max_{t,f}\|d_f(t)\|}{\max_{t,f}\|\hat{d}_f(t)\|}$
Normalized peak floor acceleration	$J_5 = \frac{\max_{t,f}\|a_f(t)\|}{\max_{t,f}\|\hat{a}_f(t)\|}$	Normalized peak control force	$J_6 = \frac{\max_t\|u_d(t)\|}{\max_t\|V_0(t)\|}$
Normalized RMS base displacement	$J_7 = \frac{\max_i\|\sigma_d(t)\|}{\max_i\|\hat{\sigma}_d(t)\|}$	Normalized RMS floors acceleration	$J_8 = \frac{\max_f\|\sigma_a(t)\|}{\max_f\|\hat{\sigma}_a(t)\|}$
Normalized energy dissipated by PFD	$J_9 = \frac{\int_0^T u_d(t)\dot{x}_b(t)dt}{\int_0^T \langle V_0(t)\dot{x}_g(t)\rangle dt}$		

f = 1,…, 5, number of floors; t = time; ∥.∥ = magnitude of vector; ⟨ ⟩ = inner product; ^ = Symbol of uncontrolled structural responses

V_0, V_1 and x_b are the base shear, structural shear and base displacement, respectively. The value of d_f, a_f and u_d are inter story drift, floors acceleration and control force, respectively. Also σ_d, σ_a, $\dot{x}_b$ and $\dot{x}_g$ are the RMS of base displacement, the RMS of floors acceleration, base velocity and ground velocity, respectively.

of ground motions are in the first 7 excitation cases and the FP component of ground motions are in the next 7 cases (which are cases 8–14).

According to Fig. 7, it can be seen that both the MPO method and the proposed AFOFPID controller result in significant reducions in J_3 and J_7 for most of earthquakes. These indices are respectively associated with the peak and RMS of base displacement. It is observed from performance indices J_5 and J_8, that the MPO of PFDs leads to a significant increase in both maximum floor acceleration and its RMS value in most earthquake case studies but the proposed controller decreases the maximum floor acceleration in all cases. As instance, the MPO of PFDs resulted in 73, 80 and 38% increase in maximum story acceleration, in comparison to the uncontrolled structure, for the El Centro-FN,

Table 8 Performance indices of various control strategies subject to earthquakes

Control method	El-Centro		Newhall		Sylmar		Rinaldi		Kobe		Chi-Chi		Erzincan	
	FP	FN	FP	FN	FP	FN	FP	FN	FP	FN	FP	FN	FP	FN
MPO														
J_1	0.60	0.58	0.53	0.95	0.62	0.69	0.62	0.88	0.75	0.77	0.67	0.65	0.76	0.80
J_2	0.78	0.59	0.74	0.99	0.65	0.71	0.63	0.91	0.80	0.84	0.68	0.65	0.76	0.70
J_3	0.24	0.28	0.30	0.74	0.5	0.60	0.52	0.75	0.49	0.57	0.55	0.59	0.59	0.70
J_4	1.00	0.71	1.00	0.99	0.65	0.71	0.63	0.91	0.94	0.86	0.68	0.65	0.79	0.80
J_5	2.31	1.73	2.35	1.80	0.77	0.77	0.72	1.07	2.56	1.38	0.81	0.68	1.53	0.87
J_6	0.59	0.51	0.42	0.22	0.19	0.13	0.16	0.15	0.35	0.25	0.18	0.09	0.21	0.12
J_7	0.16	0.18	0.17	0.62	0.29	0.41	0.34	0.54	0.43	0.59	0.47	0.49	0.34	0.51
J_8	1.60	1.59	0.95	1.41	0.50	0.51	0.50	0.86	1.69	1.69	0.68	0.55	0.61	0.61
J_9	0.93	0.94	0.91	0.83	0.82	0.74	0.80	0.77	0.87	0.82	0.56	0.63	0.86	0.74
MCO														
J_1	0.68	0.66	0.55	0.97	0.77	0.77	0.81	0.90	0.90	0.77	0.71	0.80	0.86	0.85
J_2	0.76	0.73	0.64	1.00	0.78	0.78	0.81	0.92	1.04	0.89	0.71	0.80	0.86	0.85
J_3	0.51	0.51	0.44	0.86	0.72	0.73	0.76	0.84	0.65	0.78	0.65	0.77	0.78	0.80
J_4	0.76	0.79	0.71	1.00	0.78	0.78	0.81	0.92	1.12	0.89	0.71	0.80	0.86	0.85
J_5	1.80	1.71	1.59	1.30	0.90	0.89	0.97	1.05	1.95	1.20	0.92	0.82	1.03	0.96
J_6	0.52	0.46	0.40	0.22	0.15	0.11	0.12	0.15	0.29	0.22	0.17	0.07	0.19	0.11
J_7	0.33	0.35	0.37	0.77	0.51	0.63	0.56	0.67	0.62	0.73	0.62	0.70	0.51	0.68
J_8	1.28	1.25	0.75	1.11	0.60	0.66	0.61	0.89	1.56	1.44	0.71	0.72	0.63	0.71
J_9	0.87	0.86	0.80	0.69	0.62	0.53	0.58	0.60	0.75	0.68	0.43	0.42	0.72	0.54
OPID														
J_1	0.78	0.89	0.87	0.87	0.73	0.95	0.62	0.95	0.77	0.53	0.70	0.75	0.80	0.75
J_2	0.78	0.90	0.87	0.86	0.73	0.94	0.62	0.96	0.77	0.53	0.70	0.75	0.81	0.75
J_3	0.74	0.69	0.59	0.86	0.62	0.61	0.62	0.87	0.65	0.50	0.67	0.68	0.75	0.70
J_4	0.79	0.77	0.74	0.96	0.67	0.65	0.66	1.01	0.74	0.52	0.69	0.73	0.81	0.73
J_5	0.79	0.92	0.90	0.89	0.74	0.94	0.63	1.00	0.79	0.53	0.69	0.75	0.82	0.75
J_6	0.15	0.14	0.12	0.14	0.20	0.11	0.21	0.30	0.19	0.19	0.23	0.20	0.18	0.18
J_7	0.60	0.57	0.55	0.65	0.44	0.44	0.44	0.67	0.72	0.44	0.60	0.52	0.55	0.54
J_8	0.66	0.66	0.67	0.74	0.49	0.49	0.48	0.73	0.79	0.46	0.63	0.55	0.58	0.56
J_9	0.51	0.48	0.47	0.45	0.70	0.73	0.67	0.54	0.50	0.21	0.11	0.63	0.50	0.61
SVFLC														
J_1	0.69	0.62	0.50	0.97	0.71	0.72	0.74	0.93	0.75	0.87	0.70	0.66	0.84	0.81
J_2	0.69	0.67	0.57	0.96	0.73	0.73	0.73	0.95	0.81	0.88	0.70	0.66	0.84	0.81
J_3	0.52	0.47	0.38	0.83	0.65	0.65	0.68	0.81	0.59	0.74	0.63	0.62	0.73	0.74
J_4	0.69	0.68	0.64	0.96	0.73	0.73	0.73	0.95	0.84	0.88	0.70	0.66	0.84	0.81
J_5	1.33	1.25	1.26	1.13	0.82	0.79	0.78	0.99	1.34	0.93	0.73	0.70	0.86	0.83
J_6	0.35	0.32	0.36	0.20	0.15	0.11	0.12	0.13	0.32	0.21	0.16	0.08	0.15	0.11
J_7	0.33	0.33	0.32	0.74	0.44	0.52	0.47	0.63	0.58	0.70	0.56	0.54	0.46	0.58
J_8	0.92	0.98	0.59	1.04	0.50	0.56	0.53	0.75	1.03	1.13	0.64	0.57	0.54	0.62
J_9	0.90	0.89	0.85	0.76	0.71	0.65	0.69	0.7	0.80	0.75	0.51	0.58	0.78	0.66
SOFLC														
J_1	0.63	0.60	0.51	0.98	0.68	0.70	0.71	0.91	0.71	0.85	0.70	0.69	0.83	0.79

Table 8 continued

Control method	El-Centro		Newhall		Sylmar		Rinaldi		Kobe		Chi-Chi		Erzincan	
	FP	FN	FP	FN	FP	FN	FP	FN	FP	FN	FP	FN	FP	FN
J_2	0.66	0.60	0.57	1.00	0.71	0.74	0.71	0.91	0.80	0.87	0.70	0.69	0.83	0.79
J_3	0.45	0.40	0.36	0.81	0.60	0.64	0.64	0.80	0.59	0.72	0.61	0.64	0.71	0.72
J_4	0.66	0.66	0.67	1.00	0.71	0.74	0.71	0.91	0.85	0.87	0.70	0.69	0.83	0.79
J_5	1.62	1.20	1.34	1.27	0.82	0.85	0.77	0.93	1.39	1.05	0.75	0.78	0.92	0.86
J_6	0.45	0.40	0.35	0.22	0.17	0.12	0.14	0.15	0.36	0.23	0.17	0.09	0.18	0.12
J_7	0.26	0.26	0.24	0.72	0.38	0.47	0.44	0.60	0.53	0.67	0.55	0.55	0.43	0.54
J_8	0.98	1.05	0.59	1.09	0.47	0.51	0.51	0.74	1.05	1.19	0.67	0.58	0.54	0.58
J_9	0.93	0.93	0.90	0.78	0.76	0.69	0.72	0.71	0.83	0.77	0.53	0.58	0.80	0.71
AFOFPID														
J_1	0.60	0.61	0.55	0.76	0.53	0.81	0.57	0.72	0.63	0.80	0.64	0.60	0.76	0.78
J_2	0.59	0.61	0.57	0.74	0.55	0.80	0.57	0.71	0.67	0.79	0.67	0.60	0.77	0.78
J_3	0.24	0.28	0.30	0.76	0.48	0.59	0.49	0.74	0.47	0.50	0.53	0.54	0.59	0.68
J_4	0.72	0.68	0.72	0.84	0.59	0.73	0.65	0.92	0.81	0.68	0.61	0.60	0.82	0.74
J_5	0.59	0.59	0.82	0.79	0.52	0.76	0.58	0.71	0.70	0.52	0.58	0.60	0.82	0.75
J_6	0.46	0.39	0.14	0.13	0.15	0.09	0.15	0.15	0.20	0.15	0.17	0.09	0.16	0.12
J_7	0.16	0.17	0.23	0.51	0.29	0.42	0.32	0.52	0.44	0.49	0.49	0.50	0.37	0.52
J_8	0.65	0.68	0.57	0.69	0.35	0.47	0.40	0.62	0.67	0.51	0.53	0.50	0.42	0.52
J_9	0.87	0.94	0.85	0.80	0.79	0.74	0.78	0.69	0.85	0.81	0.58	0.65	0.83	0.75

Newhall-FN and Kobe-FN earthquakes, in respective order. For the same earthquakes, however, these increases are as much as 131, 135, and 156% for the FP component. The MCO controller performs better in reduction of the maximum floor acceleration, in comparison to the MPO method, though causing deterioration in the peak isolation deformation. In addition, For the El Centro-FN, Newhall-FN and Kobe-FN earthquakes, the MCO controller results in 71, 30 and 20% increase in the maximum accelerations of floors, respectively, compared to the uncontrolled cases. These changes are 80, 59, and 95% for the FP component of mentioned earthquakes, respectively.

The SVFLC, SOFLC and OPID controllers succeed to limit the peak of floor acceleration in most earthquake excitations, while satisfactorily reducing the maximum isolator deformations, unlike the MPO and MCO methods.

Considering J_3 and J_7, it is observed that the AFOFPID controller is able to significantly decrease the maximum base displacement and its RMS value. In addition, it is concluded from comparing the performances of the AFOFPID control with those given by other control techniques that the AFOFPID controller provides the best performance in reduction of the maximum floor acceleration (J_5) and its RMS value (J_8). Compared to MPO method this controller reduced, for example, the peak floor acceleration for the El Centro-FP, Newhall-FP, Kobe-FP and Erzincan-FP earthquakes by 74, 65, 73 and 46%, respectively. Likewise, this decrease is as much as 66, 56, 62 and 14%, for the FN component of these earthquakes.

Picking the FP component of El Centro earthquake as an illustrative example, it is observed that compared to uncontrolled structure there are reductions of 48, 55 and 26% for SVFLC, SOFLC and OPID in the maximum base displacement. This reduction is
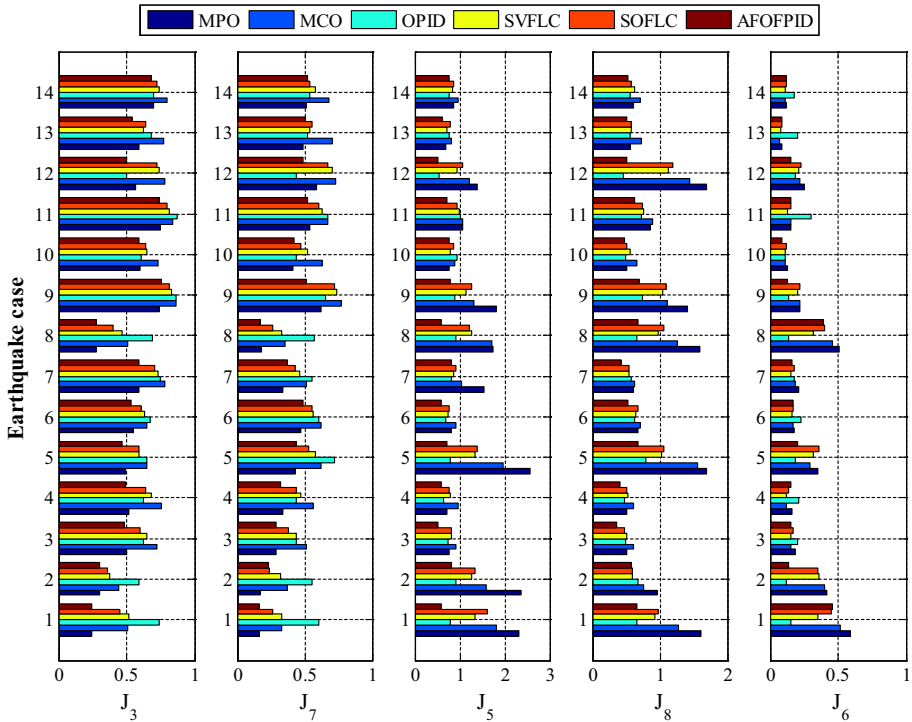
Fig. 7 Performance indices J_3, J_5, J_6, J_7 and J_8 for various control strategies

proudly 76% for AFOFPID controller. For the FN component of Chi-Chi earthquake as another example, these improvements are quantified as 38, 36, 32 and 46% for SVFLC, SOFLC, OPID and AFOFPID controllers, respectively. For the El Centro-FP and Kobe-FP earthquakes, in comparison to the uncontrolled cases SVFLC results in 33 and 34% increase in the maximum floor acceleration. In a similar fashion, these increases are 62 and 39% for SOFLC. However, OPID and AFOFPID controllers provide 21 and 41% reduction for the El Centro-FP earthquake and a reduction of 21 and 30% for the Kobe-FP earthquake. Conclusively the proposed AFOFPID controller is able to decrease two essential structural responses, namely the peak of base displacement and floor acceleration for various type of earthquakes simultaneously.

Observations made for the performance index J_6 suggest that the demanded control forces of PFD do not vary significantly between different control methods. Therefore, performance improvement is made possible without a considerable change in the level of demanding control forces. Moreover, the results of J_4, which is the performance index related to the maximum inter-story drifts, indicates that the proposed controller performs better than other control techniques specially in terms of the inter-story drifts for most earthquake case studies.

Picking the FP component of the El Centro and FN component of Chi-Chi as samples of FF and NF earthquakes, the time responses of the displacement of the isolator, top floor acceleration, command voltage and fuzzy weighing system output are shown in Figs. 8 and 9, respectively. The uncontrolled structural responses for both earthquakes are plotted on the same figure. Obviously, in case of El Centro-FP that is an FF earthquake, the proposed

controller considerably reduces the isolated building's base displacement. For an NF earthquake such as the Chi-Chi earthquake, the same result is observed as well where the maximum displacement of the base and the maximum floor acceleration of the uncontrolled system is roughly 123 cm and 8.07 m/s^2 while this value is near 66 cm and 4.84 m/s^2 for the structure controlled using AFOFPID controller. It means that the semi-active control of PFDs using the proposed controller reduces the maximum base displacement and the maximum floor acceleration by 46 and 40% in comparison to the uncontrolled structure. Figure 10 shows the hysteresis loops of isolators resulted from the passive isolation system and the AFOFPID controller, for the same FF and NF earthquake excitations. In this figure, the total shear force is the summation of the total friction and restoring force in the elastomeric bearings divided by the total weight of the structure. By applying the proposed controller to adjust the contact force of the PFDs, they increase the height and decrease the width of the hysteresis loop. In fact, PFDs decrease the displacement of the isolators, but maintain the same level of energy dissipation capacity for the isolation system by increasing the damping force.

To sum up, the AFOFPID controller is able to decrease the displacement response of the base-isolated structure in both NF and FF ground motions. Compared to other controllers, it shows a better performance in controlling the acceleration response.

The performance of the AFOFPID controller is also evaluated in the presence of an extra noise, a random Gaussian white noise. The sensitivity analysis of the system
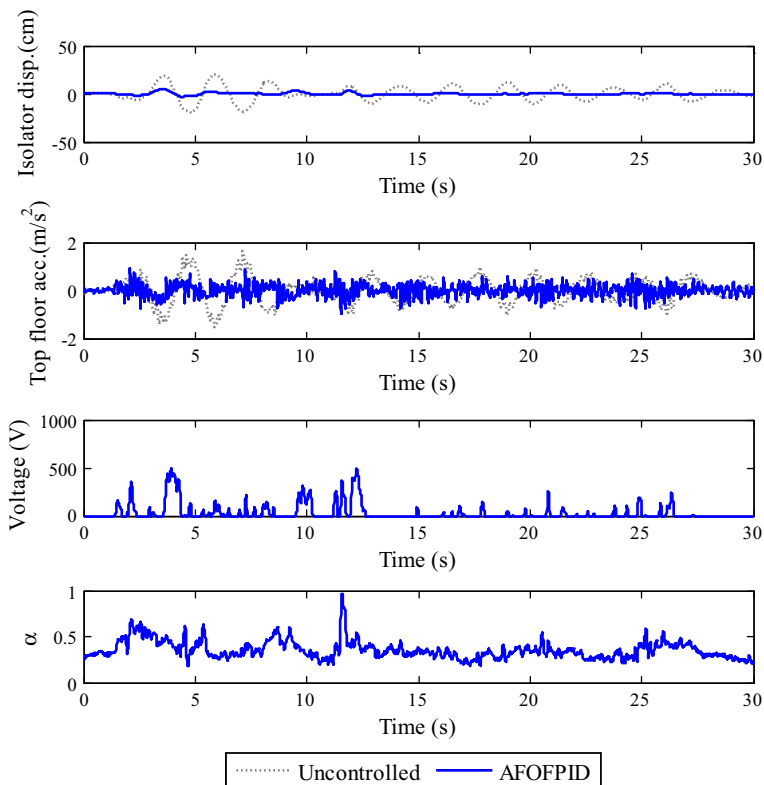

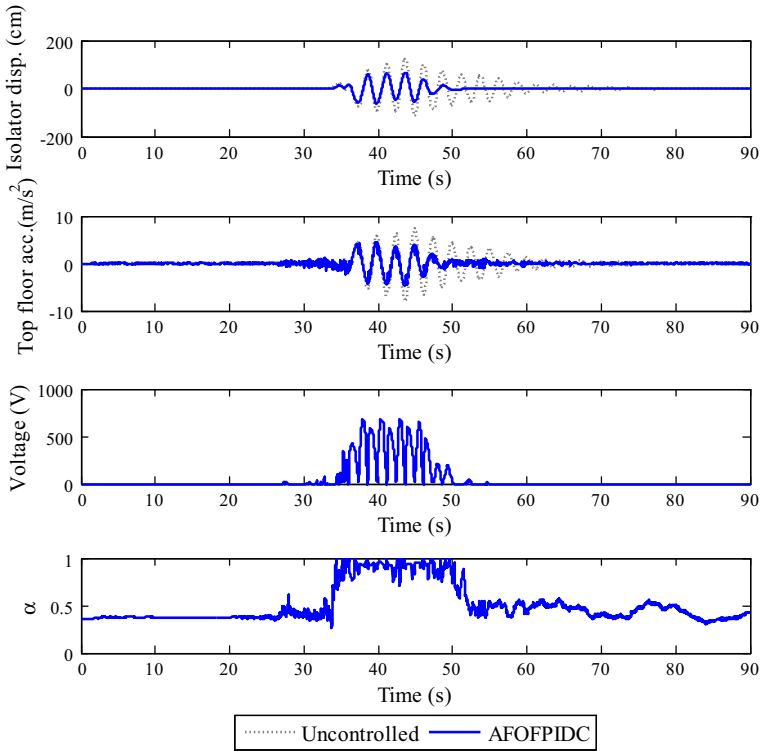Fig. 8 Time history responses of the structure subject to the El Centro-FP earthquake

Fig. 9 Time history responses of the structure subject to Chi-Chi-FN earthquake

performance is carried out and the results are shown in Table 9. A random Gaussian white noise with a variance of 10% of maximum absolute value of the ground velocity is added to the ground velocity. The results show that the maximum variation in the performance criteria is less than 3.1%.
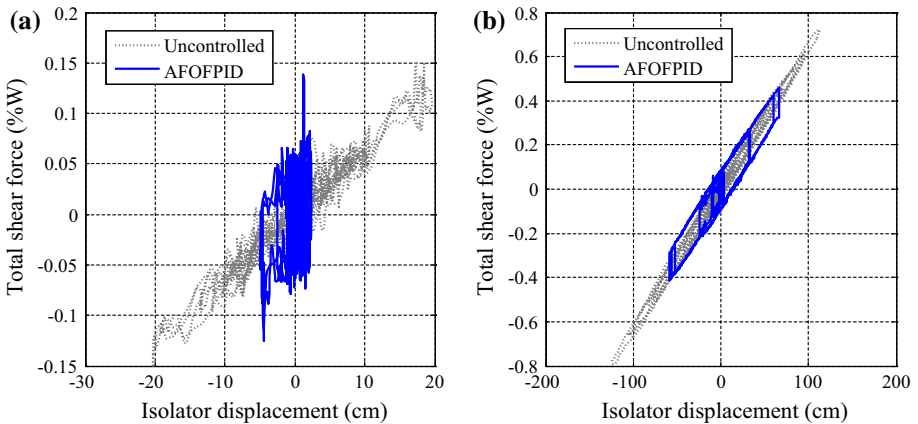

Fig. 10 Hysteresis loops of isolator for the uncontrolled and controlled structures subject to **a** El Centro-FP, **b** Chi-Chi-FN earthquakes

Table 9 Performance indices of the base-isolated building subject to artificial ground velocity

Performance indexes	J_1	J_2	J_3	J_4	J_5	J_6	J_7	J_8	J_9
Without extra noise	0.98	0.96	0.69	0.98	0.99	0.95	0.75	0.81	0.81
With extra noise	1.01	0.99	0.71	1.01	1.01	0.98	0.77	0.83	0.81

5 Conclusion

To adjust the contact force of piezoelectric friction dampers for semi-active control of base-isolated structures, an AFOFPID controller was designed. To achieve the control objectives, i.e. reduction of the isolation system deformation without allowing notable increase in the superstructure accelerations in NF and FF earthquakes, an MOCS algorithm was employed to optimize the sub-level FOFPID parameters. To enhance the performance of the sub-level FOFPID controller in facing with various earthquakes, the fuzzy rule weights of the controller were adaptively tuned according to the values of the ground velocity and top floor acceleration. Considering several control techniques, a performance comparison was carried out. It was shown that the proposed controller had a better performance in terms of simultaneous decrease of maximum base displacement and story acceleration for the given real-data earthquake excitations. Moreover, the proposed controller led to competitive responses for inter-story drifts, root mean squares of base displacements and peak floor acceleration.

References

Amini F, Mohajeri SA, Javanbakht M (2015) Semi-active control of isolated and damaged structures using online damage detection. Smart Mater Struct 24(10):105002

Arya Y, Kumar N (2016) BFOA-scaled fractional order fuzzy PID controller applied to AGC of multi-area multi-source electric power generating systems. Swarm Evolut Comput 32:202–218

Chen C, Chen G (2004) Shake table tests of a quarter-scale three-story building model with piezoelectric friction dampers. Struct Control Health Monit 11(4):239–257

Das S, Pan I, Das S, Gupta A (2012) A novel fractional order fuzzy PID controller and its optimal time domain tuning based on integral performance indices. Eng Appl Artif Intell 25(2):430–442

Etedali S, Sohrabi MR, Tavakoli S (2013) Optimal PD/PID control of smart base isolated buildings equipped with piezoelectric friction dampers. Earthq Eng Eng Vib 12:39–54

Gad S, Metered H, Bassuiny A, Abdel Ghany AM (2017) Multi-objective genetic algorithm fractional-order PID controller for semi-active magnetorheologically damped seat suspension. J Vib Control 23(8):1248–1266

Guclu R (2003) Fuzzy-logic control of vibrations of analytical multi-degree-of-freedom structural systems. Turk J Eng Environ Sci 27(3):157–167

Guclu R, Yazici H (2009) Seismic-vibration mitigation of a nonlinear structural system with an ATMD through a fuzzy PID controller. Nonlinear Dyn 58(3):553–564

Johnson EA, Ramallo JC, Spencer BF, Sain MK (1998) Intelligent base isolation systems. In: Proceedings second world conference on structural control, Kyoto, Japan, Wiley, New York, vol 1, pp 367–376

Karasakal O, Guzelkaya M, Eksin I, Yesil E, Kumbasar T (2013) Online tuning of fuzzy PID controllers via rule weighing based on normalized acceleration. Eng Appl Artif Intell 26(1):184–197

Koo B, Kwon W, Won S (2015) Active vibration control of a strip in a continuous galvanizing line using $PI^\lambda D^\mu$-type fractional-order PID controller. In: SICE annual conference 2015 July 28–30, Hangzhou, China

Lu LY, Lin GL (2009) A theoretical study on piezoelectric smart isolation system for seismic protection of equipment in near-fault areas. J Intell Mater Syst Struct 20(2):217–232

Lu LY, Lin CC, Lin GL, Lin CY (2010) Experiment and analysis of a fuzzy-controlled piezoelectric seismic isolation system. J Sound Vib 329(11):1992–2014

Mishra P, Kumar V, Rana KPS (2015) A fractional order fuzzy PID controller for binary distillation column control. Expert Syst Appl 42(22):8533–8549

Nagarajaiah S, Narasimhan S (2006) Smart base-isolated benchmark building part II: phase I, sample controllers for linear and friction isolation. Struct Control Health Monit 13(2–3):589–604

Narasimhan S, Nagarajaiah S, Johnson EA, Gavin HP (2006) Smart base-isolated benchmark building part I: problem definition. Struct Control Health Monit 13(2–3):573–588

Nauck D, Kruse R (1998) How the learning of rule weights affects the interpretability of fuzzy systems. The 1998 IEEE international conference on fuzzy systems proceedings IEEE world congress on computational intelligence. pp 1235–1240

Nigdeli SM, Boduroğlu MH (2013) Active tendon control of torsionally irregular structures under near-fault ground motion excitation. Comput-Aided Civil Infrastruct Eng 28(9):718–736

Oustaloup A, Levron F, Mathieu B, Nanot FM (2000) Frequency-band complex noninteger differentiator: characterization and synthesis. IEEE Trans Circuits Syst I: Fundam Theory Appl 47(1):25–39

Ozbulut OE, Hurlebaus S (2010) Fuzzy control of piezoelectric friction dampers for seismic protection of smart base isolated buildings. Bull Earthq Eng 8:1435–1455

Ozbulut OE, Bitaraf M, Hurlebaus S (2011) Adaptive control of base-isolated structures against near-field earthquakes using variable friction dampers. Eng Struct 33(12):3143–3154

Rajabioun R (2011) Cuckoo optimization algorithm. Appl Soft Comput 11:5508–5518

Sharma R, Rana KPS, Kumar V (2014) Performance analysis of fractional order fuzzy PID controllers applied to a robotic manipulator. Expert Syst Appl 41(9):4274–4289

Song G, Sethi V, Li HN (2006) Vibration control of civil structures using piezoceramic smart materials: a review. Eng Struct 28(11):1513–1524

Yang XS, Deb S (2009) Cuckoo search via Lévy flights. In: The world congress on nature and biologically inspired computing (NaBIC), pp 210–214

Yang XS, Deb S (2013) Multi objective cuckoo search for design optimization. Comput Oper Res 40:1616–1624

Zamani AA, Tavakoli S, Etedali S (2017) Control of piezoelectric friction dampers in smart base-isolated structures using self-tuning and adaptive fuzzy proportional–derivative controllers. J Intell Mater Syst Struct 28(10):1287–1302

Zhao D, Li Y (2015) Fuzzy control for seismic protection of semiactive base-isolated structures subjected to near-fault earthquakes. Math Problems Eng. https://doi.org/10.1155/2015/675698